View metadata, citation and similar papers at core.ac.uk
brought to you by CORE
provided by Digital.CSIC

Positioning tolerances for phase plates compensating aberrations of the human eye

Salvador Bará, Teresa Mancebo, and Esther Moreno-Barriuso

The positioning tolerances for phase plates used to compensate human eye aberrations are analyzed. Lateral displacements, in-plane rotations, and axial translations are considered, describing analytic and numerical procedures to compute the maximum degree of compensation achievable in each case. The compensation loss is found to be dependent both on the kind and the amount of misalignment and on the particular composition of the aberration pattern of each subject in terms of Zernike polynomials. We applied these procedures to a set of human eye aberrations measured with the laser ray-tracing method. The general trend of results suggests that lateral positioning, followed by angular positioning, are the key factors affecting compensation performance in practical setups, whereas axial positioning has far less stringent requirements. © 2000 Optical Society of America

OCIS codes: 220.1000, 330.4460, 080.1010, 080.2740, 170.0110.

1. Introduction

In recent years we have witnessed a growing interest in techniques for measuring and compensating the wave aberrations of the human eye beyond classical ametropia. The efficient correction of those aberrations opened exciting fields of applications, among them the improvement of visual acuity and the *in vivo* high-resolution imaging of the mosaic of photoreceptors in the retina; it can be anticipated that they will likely allow for other relevant breakthroughs in ocular correction and vision science.

All compensating procedures make use of some kind of optical element encoding a phase conjugated to the wave aberration of the eye. Different technologies have been proposed and implemented to manufacture those correcting elements. A partial compensation of specific eye aberrations, e.g., third-order spherical and coma, has been performed with radially symmetrical lenses.[1,2] Compensation of the wave aberration, not restricted to specific Seidel terms, has been reported with use of deformable mirrors[3,4] and also liquid-crystal spatial light modulators.[5,6] Recently, a novel technique for designing and fabricating general compensating phase plates by single-mask photosculpture of photoresist has been demonstrated.[7,8] In this technique the desired phase is encoded as a continuous refractive profile of photoresist on a glass substrate, with high spatial resolution, low cost, and good reproducibility. The reported results showed ~80% aberration compensation both in an artificial and a living eye.

A key factor for achieving the optimum degree of compensation is the proper positioning of the correcting element in the reference frame for which it was designed, usually coincident with a conjugate of the eye's pupil. However, in any experimental setup some misalignments can occur, reducing in this way the performance of the compensating system.

In this paper we study the loss of compensation suffered when a well-matched ocular correcting plate is displaced (either axially or transversally) or rotated with respect to its reference position. Although we will specifically refer to refractive plates like those described in Refs. 7 and 8, the calculation procedures and overall results reported here are applicable—directly or with few modifications—to most of the compensating elements proposed to date. They represent an upper limit for the expected performance of a misaligned system and provide procedures to evaluate positioning tolerances for practical cases.

As expected, the compensation loss is dependent on the specific aberration pattern of each subject as well

S. Bará (bara@usc.es) and T. Mancebo are with the Área de Óptica, Facultade de Física, Universidade de Santiago de Compostela, 15706 Santiago de Compostela, Galicia, Spain. E. Moreno-Barriuso is with the Instituto de Óptica "Daza de Valdés," Consejo Superior de Investigaciones Científicas, Serrano, 121, 28006 Madrid, Spain.

Received 4 January 2000; revised manuscript received 30 March 2000.
0003-6935/00/193413-08$15.00/0
© 2000 Optical Society of America

as on the amount and the type of misalignment. To get insight about the magnitude and the behavior of this dependence for human eyes, the general expressions derived here were applied to the ocular aberrations of several subjects measured *in vivo* with the laser ray-tracing technique.[9,10] The results show that transversal positioning is a critical parameter to be controlled carefully in any compensation setup, whereas slightly less stringent requirements affect both in-plane rotations and axial displacements.

In Section 2 we present the main assumptions of the model used to evaluate the compensation loss. In Section 3 the effects of lateral displacements are evaluated. Section 4 deals with angular misalignments that are due to in-plane rotations of the compensating plate, whereas the somewhat more complex analysis of axial displacements is described in Section 5. The application of these results to aberration data of the human eye is carried out in Section 6.

2. Degree of Compensation

Let $W_e(\mathbf{r})$ be the wave aberration of an eye, expressed as a linear combination of Zernike polynomials,

$$W_e(\mathbf{r}) = \sum_{i=1}^{M} a_i Z_i(\mathbf{r}/R), \tag{1}$$

where $Z_i(\mathbf{r}/R)$ is the ith Zernike mode defined following Ref. (11), R is the pupil radius, and M is the number of modes included in the expansion of $W_e(\mathbf{r})$. Henceforth we will consider $W_e(\mathbf{r})$ to be an optical path length (OPL) so that both $W_e(\mathbf{r})$ and the modal coefficients $a_i (i = 1, \ldots, M)$ will be expressed in units of length. Note that in Ref. (11) the Zernike terms are defined such that the maximum value of any Z_i at the pupil border equals 1; a_i then represents the maximum OPL deviation at the pupil rim associated to each specific aberration with respect to the reference wave front.

Let $W_p(\mathbf{r})$ be the OPL introduced by a correcting plate designed to compensate this aberration. We assume that this plate can be treated as a thin optical element whose role is to add a local phase retardation to the incoming wave fronts. Since we are interested in studying the absolute upper limits of the compensation performance after misalignment of this plate, we will assume that it is free from manufacturing errors so that, when properly placed in the compensating setup, we have $W_p(\mathbf{r}) = -W_e(\mathbf{r})$ for points inside the eye pupil. Throughout this study we will assume that the compensating plates are fabricated by photosculpture of photoresist deposited onto a wider transparent glass substrate so that $W_p(\mathbf{r}) = 0$ (or, in general, any constant value) for points lying outside the circular plate pupil ($r > R$).

In the case of misalignments the resulting wave front produced by the plate at the eye pupil will be denoted by $W'_p(\mathbf{r})$. The residual eye aberration after compensation with this misaligned plate will then be

$$W_r(\mathbf{r}) = W_e(\mathbf{r}) + W'_p(\mathbf{r}). \tag{2}$$

The degree of compensation is defined as

$$D = 1 - \sigma_r/\sigma_e, \tag{3}$$

where

$$\sigma_r = \left[\frac{1}{\pi R^2}\int W_r^{\,2}(\mathbf{r})\mathrm{d}^2\mathbf{r}\right]^{1/2} \tag{4}$$

is the rms variance of the residual wave front and

$$\sigma_e = \left[\frac{1}{\pi R^2}\int W_e^{\,2}(\mathbf{r})\mathrm{d}^2\mathbf{r}\right]^{1/2} \tag{5}$$

is the original rms eye aberration. The integral extends in both cases to the eye pupil area.

For a perfect compensation we have $D = 1$, whereas $D = 0$ represents the original aberrated eye. Intermediate values of D account for partial compensation situations. Note that D can also take negative values, indicating a residual aberration higher than the original aberration of the eye, a situation that can appear in cases of strong misalignment of the compensating plates.

The Zernike polynomials can be normalized as[12]

$$\hat{Z}_i(\mathbf{r}/R) = c_i Z_i(\mathbf{r}/R), \tag{6}$$

with $c_i \equiv c_{n,l} = [(2 - \delta_{l0})(n + 1)]^{1/2}$ where n and l are the radial and the azimuthal degrees, respectively, of the ith polynomial and δ is the Kronecker delta. They then become orthonormal in the circle of radius R obeying

$$\frac{1}{\pi R^2}\int \hat{Z}_i(\mathbf{r}/R)\hat{Z}_j(\mathbf{r}/R)\mathrm{d}^2\mathbf{r} = \delta_{ij}. \tag{7}$$

Expanding W_e, W'_p, and W_r in terms of the normalized Zernike polynomials with coefficients $\hat{a}_i$, $\hat{a}'_i$, and $\hat{a}_{ir}$, respectively, we can write the degree of compensation as

$$D = 1 - \left[\frac{\sum_{i=1}^{M}(\hat{a}_i + \hat{a}'_i)^2}{\sum_{i=1}^{M}\hat{a}_i^{\,2}}\right]^{1/2} = 1 - \left[\frac{\sum_{i=1}^{M}\hat{a}_{ir}^{\,2}}{\sum_{i=1}^{M}\hat{a}_i^{\,2}}\right]^{1/2}, \tag{8}$$

where the normalized modal coefficients are related to the nonnormalized ones [Eq. (1)] by $\hat{a}_i = c_i^{-1} a_i$, $\hat{a}'_i = c_i^{-1} a'_i$, $\hat{a}_{ir} = c_i^{-1} a_{ir}$.

3. Lateral Displacements

The case of a lateral displacement $\mathbf{d}$ of the compensating plate with respect to the center of the eye pupil is schematically depicted in Fig. 1. The overlapping region of the plate and eye pupils, $P1$, is partially compensated [$W_r(\mathbf{r}) = W_e(\mathbf{r}) + W'_p(\mathbf{r})$], whereas the region $P2$ remains totally uncompensated [$W_r(\mathbf{r}) =$

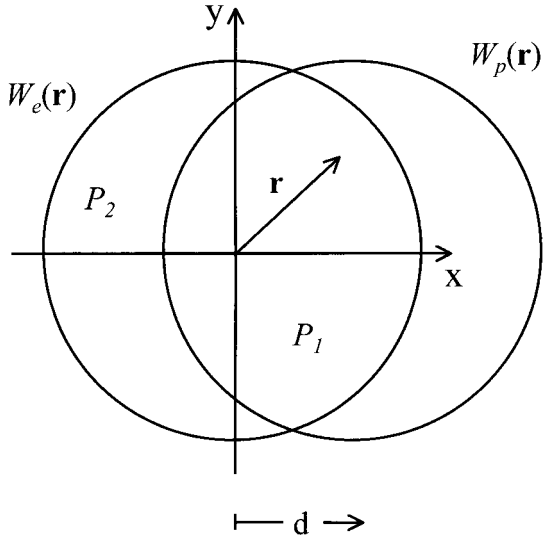

Fig. 1. Laterally displaced correcting phase plate. $W_e(\mathbf{r})$, eye aberration; $W_p(\mathbf{r})$, plate OPL; P_1, region of overlapping pupils; P_2, uncompensated eye pupil area.

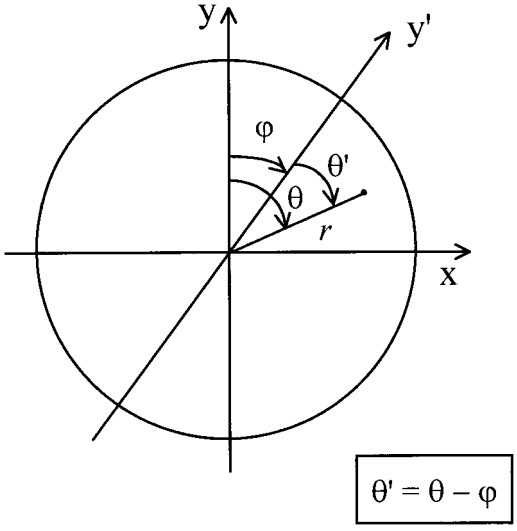

Fig. 2. In-plane rotated correcting phase plate.

$W_e(\mathbf{r})]$. The variance of the residual aberration is then given by

$$\sigma_r^2 = \frac{1}{\pi R^2}\int_{P1}[W_e(\mathbf{r}) - W_e(\mathbf{r}-\mathbf{d})]^2 d^2\mathbf{r} + \frac{1}{\pi R^2}\int_{P2} W_e^2(\mathbf{r}) d^2\mathbf{r}. \quad (9)$$

For small displacements the integrand in $P1$ can be expanded in powers of $\mathbf{d}$, to obtain the residual wave front as $W_r(\mathbf{r}) \approx \nabla W_e(\mathbf{r}) \cdot \mathbf{d}$. But even with this approximation, when we evaluate analytically σ_r^2 with this expression, we face some difficulties that are due to the shape of the borders of regions $P1$ and $P2$. It turns out to be more advisable to evaluate Eq. (9) directly by some numerical routine. Since, in practice, the eye aberration is expanded up to a relatively low radial and azimuthal degree (say $n, l = 7$, with 35 Zernike terms), a quite good evaluation of σ_r^2 can be done by means of computing the average squared residual aberration in a sufficiently dense grid of points $\mathbf{r}_\alpha(\alpha = 1 \text{ to } N)$ as

$$\sigma_r^2 = N^{-1}\sum_{\alpha=1}^{N}[W_e(\mathbf{r}_\alpha) + W_p(\mathbf{r}_\alpha)]^2, \quad (10)$$

taking $W_p(\mathbf{r}_\alpha) = -W_e(\mathbf{r}_\alpha - \mathbf{d})$ for points $\mathbf{r}_\alpha$ located inside the eye pupil and zero otherwise.

Note that for most practical applications the piston term of the original and the residual aberrations is not relevant, and the tilt terms simply account for a lateral translation of the images without affecting their overall quality. A lateral displacement of the correcting plate will give rise, among other effects, to additional tilt terms coming from the order-of-2 powers in W_e. If one is interested mainly in evaluating the degree of compensation of the aberrations relevant to influencing the image quality, both the global piston and tilts can be excluded from the original and the residual aberrations before one proceeds to evaluate D.

Finally, let us point out that the assumption of $W_p(\mathbf{r}) = 0$ for points with $r > R$ represents a worst-case situation, assuming that the correction plate compensates only variable phases in a circular region with the same size as the eye pupil. It seems possible in principle to extend the plate transmittance function outside this region such that the aberration in the integral $P2$ [Eq. (9)] is at least partially compensated for a certain range of lateral displacement. This possibility, however, is not studied here in detail.

4. In-Plane Rotations

The situation arising from in-plane rotations of the compensating plate with respect to the eye pupil is represented in Fig. 2, with the notation of Ref. (11). The residual wave front in polar coordinates $\mathbf{r} = (r, \theta)$ is then given by

$$W_r(r, \theta) = W_e(r, \theta) - W_e(r, \theta - \phi) \quad (11)$$

where ϕ is the rotation angle. The degree of compensation can be computed accurately in this case by a finite sum from σ_r^2 as in Eq. (10). However, the rotational symmetry properties of the Zernike polynomials allow us to obtain an analytical formula for D in terms of the normalized modal coefficients of the original eye aberration $\hat{a}_i$.

To derive this formula, let us recall that the normalized Zernike polynomials can be written as

$$\hat{Z}_i(\mathbf{r}/R) \equiv \hat{Z}_{n,l}(\mathbf{r}/R) = c_{n,l}\mathbf{R}_n^{\,l}(r/R)A_l(\theta), \quad (12)$$

where $R_n^{\,l}$ is the radial part of $\hat{Z}_{n,l}$ (verifying $R_n^{\,l} = R_n^{\,-l}$) and $A_l(\theta)$ is the angular one, given by[11]

$$\begin{aligned} A_l(\theta) &= \cos(l\theta), & l < 0 \\ &= \sin(l\theta), & l > 0 \\ &= 1, & l = 0. \end{aligned} \quad (13)$$

The eye aberration can then be expressed as

$$W_e(\mathbf{r}) = \sum_{n=1}^{N_m} \sum_{l=-n}^{n} \hat{a}_{n,l} c_{n,l} R_n^{\,l}(r/R) A_l(\theta) \tag{14}$$

with n and l obeying the usual restriction of having the same parity.[13] Rearranging Eq. (14), we get

$$W_e(r, \theta) = \sum_{n=1}^{N_m} \sum_{l\geq 0}^{n} c_{n,l} R_n^{\,l}(r/R)[\hat{a}_{n,-l} \cos(l\theta) + \hat{a}_{n,l} \sin(l\theta)] \tag{15}$$

Now, by direct substitution it is easy to show that the rotated aberration $W_e(r, \theta - \phi)$ can be written as

$$W_e(r, \theta - \phi) = \sum_{n=1}^{N_m} \sum_{l\geq 0}^{n} c_{n,l} R_n^{\,l}(r/R)[\hat{a}'_{n,-l} \cos(l\theta) + \hat{a}'_{n,l} \sin(l\theta)], \tag{16}$$

where the new modal coefficients are related to the original ones by

$$\begin{pmatrix} \hat{a}'_{n,l} \\ \hat{a}'_{n,-l} \end{pmatrix} = \begin{bmatrix} \cos(l\phi) & \sin(l\phi) \\ -\sin(l\phi) & \cos(l\phi) \end{bmatrix} \begin{pmatrix} \hat{a}_{n,l} \\ \hat{a}_{n,-l} \end{pmatrix}. \tag{17}$$

The transformation depends exclusively on the rotation angle ϕ as well as on the azimuthal degree l of the Zernike term, but it is independent from the radial degree n. The above expression can be written in vector form as

$$\hat{\mathbf{a}}'_{nl} = M(l\phi)\hat{\mathbf{a}}_{nl}, \tag{18}$$

where $\hat{\mathbf{a}}_{nl}$ stands for any two-dimensional column vector of Zernike coefficients with the same n and opposite sign l and $M(l\phi)$ is the rotation matrix. From Eq. (11) the n,l modal coefficients vector of the residual wave front, $\hat{\mathbf{a}}_{nl}{}^{r}$, is then given by

$$\hat{\mathbf{a}}_{nl}{}^{r} = [I - M(l\phi)]\hat{\mathbf{a}}_{nl}, \tag{19}$$

where I is the identity matrix. Now, taking into account that Eq. (8) can be rewritten as

$$D = 1 - \left[\frac{\sum_{n=1}^{N_m} \sum_{l\geq 0}^{n} |\hat{\mathbf{a}}_{nl}{}^{r}|^2}{\sum_{n=1}^{Nm} \sum_{l\geq 0}^{n} |\hat{\mathbf{a}}_{nl}|^2} \right]^{1/2}, \tag{20}$$

where $|\hat{\mathbf{a}}_{nl}|^2 = \hat{a}_{n,l}{}^2 + \hat{a}_{n,-l}{}^2$ (and the corresponding similar expression holds for $|\hat{\mathbf{a}}_{nl}{}^{r}|^2$), we finally get

$$D = 1 - \left[\frac{\sum_{n=1}^{Nm} \sum_{l\geq 0}^{n} [1 - \cos(l\phi)]|\hat{\mathbf{a}}_{nl}|^2}{\sum_{n=1}^{Nm} \sum_{l\geq 0}^{n} |\hat{\mathbf{a}}_{nl}|^2} \right]^{1/2}. \tag{21}$$

Equation (21) provides the maximum degree of compensation attainable with a rotated correcting plate. Note that the numerator is simply a modified version of the denominator, with each $|\hat{\mathbf{a}}_{nl}|^2$ term weighted by the factor $[1 - \cos(l\phi)]$, which accounts for the increased sensitivity to rotations of modes with higher l-fold symmetry. Note also that the rotationally symmetric aberrations ($l = 0$) make no contribution to decreasing D.

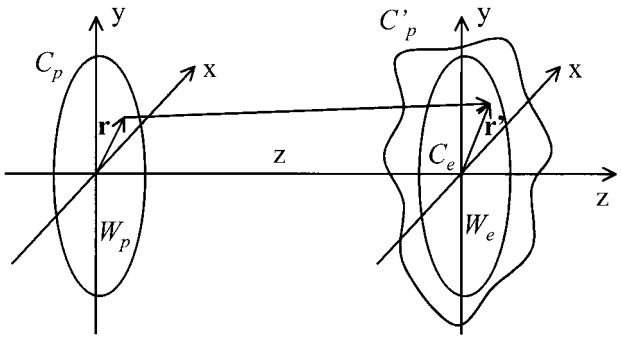

Fig. 3. Axially displaced correcting phase plate.

For small rotation angles, as is the usual case in misaligned setups, we can set $\cos(l\phi) \approx 1 - l^2\phi^2/2$, and Eq. (21) simplifies to

$$D = 1 - |\phi| \left[\frac{\sum_{n=1}^{Nm} \sum_{l\geq 0}^{n} l^2 |\hat{\mathbf{a}}_{nl}|^2}{\sum_{n=1}^{Nm} \sum_{l\geq 0}^{n} |\hat{\mathbf{a}}_{nl}|^2} \right]^{1/2}, \tag{22}$$

indicating that for small ϕ the degree of compensation decreases linearly with the absolute value of the rotation angle, with a slope given by the bracket factor. Again, the modal terms with higher l are more strongly weighted, indicating that a worse relative compensation shall be expected for rotated plates corresponding to aberrated eyes in which high-l aberrations contribute substantially to the whole aberration function.

5. Axial Displacements

Axial displacements of the correcting plate (Fig. 3) also give rise to a decrease in the degree of correction.

There are several possibilities for computing $W'_p(\mathbf{r})$, i.e., the OPL correction provided at the eye pupil by an axially displaced plate $W_p(\mathbf{r})$ illuminated by an on-axis point source at infinity and located at a distance z from its nominal position. The direct approach, although computationally expensive, is to evaluate the Fresnel diffraction integral numerically for the propagation between the two planes.[14] Nevertheless, since in practical situations of eye aberration correction the waves exiting the correcting plate are not expected to focus or give rise to caustic areas in the range of z of interest, a first-order nonuniform asymptotic expansion of the diffraction integral will provide quite accurate results.[15] In this approach, essentially a geometrical optics one, neglecting diffraction at the plate pupil border and restricting ourselves to the paraxial approximation, the OPL at points $\mathbf{r}'$ in the eye pupil produced by the axially displaced plate is given by

$$W'_p(\mathbf{r}') = W_p(\mathbf{r}) + z + \left(\frac{1}{2z}\right)|\mathbf{r}' - \mathbf{r}|^2, \tag{23}$$

where the constant additive term z can be dropped, since it contributes only to the global piston. In Eq. (23) $\mathbf{r}$ stands for the point(s) inside the plate pupil for which the phase at $\mathbf{r}'$ is stationary. This condition provides the mapping connecting $\mathbf{r}$ and $\mathbf{r}'$, which determines the ray trajectories between the two planes

$$\mathbf{r}' = \mathbf{r} + z\nabla W_p(\mathbf{r}). \tag{24}$$

Equations (23) and (24) allow us to calculate W'_p at any arbitrary set of points $\mathbf{r}'$ in the eye pupil. However, to do so it becomes necessary to solve Eq. (24) backwards for finding the stationary point $\mathbf{r}$ associated to each $\mathbf{r}'$. Solving this equation is not always practical, since for each component of $\mathbf{r}'$ it involves sums of products with powers of x and y up to the $(n-1)$th degree, arising from the gradient of W_p. Although the desired solutions can be found by numerical calculus, in practice this is not necessary. A slightly different and more convenient practical approach is to use Eq. (24) in a forward way, with the following steps:

1. Define a sufficiently dense grid of sampling points $\mathbf{r}_\alpha(\alpha = 1, \ldots, N)$ inside the pupil of the correcting plate.
2. Propagate them to the eye's pupil plane with Eq. (24) to find the corresponding impact points $\mathbf{r}'_\alpha$; exclude those points falling outside the eye pupil.
3. Compute $W'_p(\mathbf{r}'_\alpha)$ with Eq. (23).
4. Calculate the degree of correction D either (a) by use of Eq. (3) with

$$\sigma_r{}^2 \simeq N^{-1} \sum_{\alpha=1}^{N} [W_e(\mathbf{r}'_\alpha) + W'_p(\mathbf{r}'_\alpha)]^2,$$
$$\sigma_e{}^2 \simeq N^{-1} \sum_{\alpha=1}^{N} [W_e(\mathbf{r}_\alpha)]^2 \tag{25}$$

or (b) in a modal way, by calculating the normalized Zernike coefficients of W'_p by a least-squares fit[16,17] of

$$W'_p(\mathbf{r}) = \sum_{i=1}^{M} \hat{a}'_i \hat{Z}_i(\mathbf{r}/R) \tag{26}$$

to the set of $W'_p(\mathbf{r}'_\alpha)$ data and finding D with Eq. (8).

Some remarks have to be taken into account when we apply these procedures. First, the grid $\mathbf{r}_\alpha$ has to provide both for a dense sampling of the plate pupil and for a dense sampling (by means of $\mathbf{r}'_\alpha$) of the eye pupil to get accurate values for $\sigma_r{}^2$ and $\sigma_p{}^2$ with relation (25) or $\hat{a}'_i$ with Eq. (26). In fact, this is not a practical limitation, since many available software packages can handle reasonably sized sampling grids at low computational cost. As an order-of-magnitude example, a square grid of size 250×250 including a circular pupil of 250 pixels in diameter allows for an effective sampling of the wave aberrations in more than 48,600 points with a spatial period of $R/125$ (e.g. 24 μm for a 6-mm-diameter pupil), which more than enough to capture all relevant features of the wave fronts under study ($n \leq 7$). Second, when we start from an evenly spaced grid $\mathbf{r}_\alpha$, an uneven, slightly deformed $\mathbf{r}'_\alpha$ grid is obtained. Again, this is not a significant problem, since the grid deformation is directly proportional to the translation distance z, which can be expected to be small for any practical application. Finally, and related to this last fact, it must be taken into account that the plate pupil border C_p is mapped by means of Eq. (24) to a modified border C'_p in the eye pupil plane. If the radial component of $\nabla W_p(\mathbf{r})$ is positive everywhere at C_p, then C'_p will encircle C_e. Otherwise this mapping will give rise to a smaller effective area of the eye pupil over which compensation will be performed. The difference between C'_p and C_e is of little concern for small z displacements, but it can produce noticeable effects as z increases.

Regarding the potential differences to be obtained with step 4(a) or 4(b) to compute D, they are in general of little practical concern. Working with actual data of eye aberrations (see Section 6) both methods give nearly coincident results (within 0.2%) for displacements z up to several pupil radii R.

6. Application to Human Eye Aberrations

The expressions and procedures presented in the previous sections provide a general framework for estimating the effects of misalignments and positioning errors of the correcting plates. As stated, the decrease of D depends not only on the kind and amount of misplacement but also on the particular composition of the eye aberration in terms of Zernike polynomials. In practice, any definite assessment of the positioning tolerances for a given correcting plate has to be made in a case-based approach, taking into account the particular aberration to be compensated for. To exemplify the utility of these methods and to get some insight about the general behavior of D, we find it useful to apply them to some set of actual eye aberration data.

In this section we present the numerical results corresponding to the eye aberrations of three subjects, measured by the laser ray-tracing method at the Instituto de Optica, Consejo Superior de Investigaciones Científicas, Madrid.[9,10] Measurements were performed under mydriasis and cycloplegia by instillation of two drops of cyclopentolate 1%, with zero-diopter accommodation. The effective sampled pupil diameter was 6.5 mm. The corresponding fitted Zernike coefficients are listed in Table 1. They correspond to the unnormalized coefficients a_i appearing in Eq. (1) and are given in micrometers. Since neither piston nor tilt is of concern here, coefficients 0, 1, and 2 are not listed in this table. The overall rms wave-front aberration is 1.18, 2.11, and 5.13 μm for subjects A, B, and C, respectively. The modal composition of the aberration function is also largely different from one to another.

In Fig. 4 we plot the degree of compensation D versus the lateral displacement of the correcting plate d, measured in units R (pupil radius), for displacements along the x and the y directions with residual tilt removed. The curves follow a similar pattern, although the particular preeminence of some aberrations gives rise to distinct compensation effi-

Table 1. Zernike Aberration Coefficients of Subjects A–C for Modes $i = 3$–35

i	A	B	C
3	1.11	0.27	−2.75
4	−1.31	−3.57	−6.98
5	−1.69	−0.62	−6.17
6	−0.51	−0.22	0.91
7	−0.24	0.22	−0.30
8	−0.47	0.06	2.22
9	−0.60	−0.71	−1.63
10	0.06	−0.07	1.11
11	0.07	0.11	−0.12
12	0.00	−0.49	−2.15
13	−0.11	0.22	−0.26
14	−0.10	0.08	0.32
15	0.37	0.13	−0.09
16	−0.06	−0.05	0.05
17	0.04	0.18	−0.03
18	0.15	0.10	0.50
19	−0.12	0.20	−0.41
20	−0.06	0.09	1.53
21	0.03	0.01	−0.39
22	−0.07	−0.02	0.22
23	0.09	0.04	−0.34
24	0.05	−0.07	−0.28
25	0.01	0.01	0.21
26	0.03	0.02	−0.07
27	−0.04	0.07	−0.20
28	−0.01	0.02	−0.50
29	−0.03	−0.08	−0.36
30	−0.03	0.04	−0.18
31	−0.08	−0.10	0.31
32	0.01	−0.11	0.22
33	−0.08	−0.06	−0.31
34	0.00	0.02	0.40
35	0.06	−0.07	0.08

ciencies: e.g., subjects A and C, with a noticeable astigmatic component along the y direction ($i = 5$) suffer a strong compensation loss for displacements of the correcting plate along this axis and a clearly smaller relative loss for displacements along the orthogonal one. Subject B, with a predominantly symmetrical aberration pattern of defocusing ($i = 4$) and spherical aberration ($i = 12$), shows an essentially similar performance for displacements along both axes.

From these data, compensation degrees higher than 0.8 can reasonably be expected for these subjects if the correcting plates are kept laterally centered up to approximately $0.008–0.016\ R$, which corresponds to 26–52 μm. Although this accuracy is well inside the standard positioning capabilities of any fairly equipped laboratory, it puts a stringent requirement on the optomechanical stability of optical setups designed to measure and compensate *in vivo* eye aberrations.

The dependence of D on rotations is shown for the same subjects in Fig. 5(a), for ϕ between 0 and 360 deg, and in more detail in Fig. 5(b) for ϕ between −15 and +15 deg, both plotted with Eq. (21). The degree of compensation oscillates, attaining a minimum

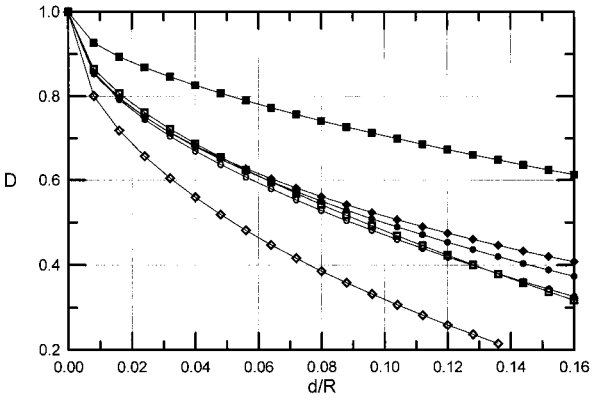

Fig. 4. Degree of compensation D versus normalized lateral displacement d/R of the correcting plate. Tilt has been removed from the residual aberration. Plots for displacements along the X axis: subjects A (filled squares), B (filled circles), C (filled diamonds). Displacements along the y axis: A (open squares), B (open circles), C (open diamonds).

value that can be not only zero but even negative if the rotationally symmetrical aberrations ($i = 4$, 12, 24) play a small relative role (subjects A and C). The position and the level of this minimum depend on the particular aberration pattern, and in this example they correspond to $D = -0.47$ at $\phi = 90$ deg (subject A), $D = 0.64$ at $\phi = 70$ deg, (subject B), and $D = -0.12$ at $\phi = 90$ deg (subject C). The nearly symmetrical aberration pattern of subject B makes it remain relatively well compensated for any angular shifting of the correcting plate. As expected from Eq. (21) all plots are symmetrical with respect to $\phi = 180$ deg.

For small rotation angles [Fig. 5(b)] a nearly linear relationship is found, in agreement with the approximate Eq. (22). The different slopes (−0.0285, −0.0085, and $-0.0221\ \text{deg}^{-1}$ for A, B, and C, respectively) reflect the relative weight of high azimuthal-order modes in each aberration. A compensation level of $D = 0.8$ is within reach if the angular positioning system allows us to keep the plate aligned within approximately ±7 deg (subject A), ±9 deg (subject C), and—as expected—a substantially wider region of approximately ±25 deg for subject B.

Finally, D is plotted in Fig. 6 versus the axial z displacement, measured in units R. The calculation was performed following the procedure in step 4(b), stated in Section 5, with the modal approach of Eqs. (8) and (26). The alternative way in step 4(a) with relations (3) and (25) gives essentially the same results, well within a 0.2% difference in the worst case. The small amount of residual tilt originating from wave propagation has been removed (it contributes with a mere 0.01 to the value of D in the range of z considered).

Apart from obvious individual differences, it can be seen that quite reasonable compensation values (>0.95) are attainable even for moderately high displacements, provided that the eye aberration (and hence the compensating plate) did not have strong

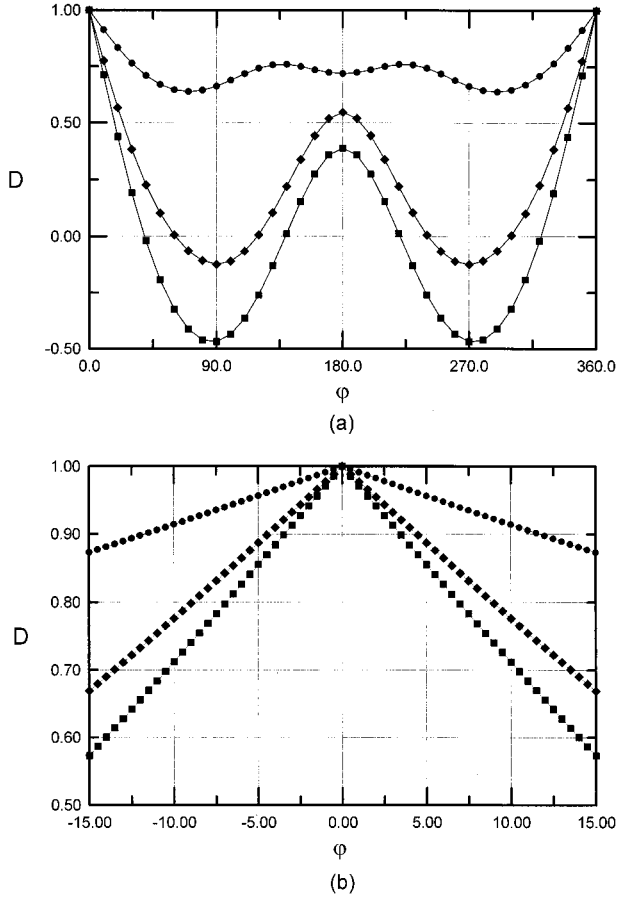

Fig. 5. Degree of compensation D versus in-plane rotation angle ϕ (degrees) of the correcting plate for aberrations corresponding to subjects A (squares), B (circles), C (diamonds). (a) Range, 0–360 deg; (b) Range, −15–15 deg.

local wave-front curvatures. The relative level of the compensation loss for each subject correlates well with the expected overall divergence of the wave fronts exiting the correcting plate (see, e.g., coefficients $i = 4$, 12, and 24, taking into account that they correspond to the eye aberration and that the correcting plate OPL has the opposite sign).

Although in no way meant to be representative of the whole range of living eye aberrations, the previous results allow us to advance the notion that for practical compensation setups lateral positioning and, to a lesser degree, angular positioning are probably the key factors affecting the compensation efficiency, given the relatively narrow limits within which we have to move. Axial positioning is noticeably less stringent.

The procedures developed here can be applied to the particular case of compensation of classical spherocylindrical ametropia, described by a combination of the low-order aberrations defocus ($n = 2$, $l = 0$) and astigmatism ($n = 2$, $l = \pm 2$), obtaining already known results. For instance, it is straightforward to check that small axial shifts in conventional spectacle lenses do not cause a significant degradation of compensation. Lateral displacements give rise to residual tilts, and the astigmatic error (measured as the residual wave-front variance associated to astigmatic terms) arising from a rotated cylindrical lens is proportional to the squared sinus of the rotation angle, as can be deduced from Eq. (19).

Out-of-plane rotations of the correcting plate (tilts around the X or the Y axis) will also affect the degree of compensation, although they are relatively easy to detect and correct in practical setups when we use the light reflected by the plate. This case, as well as the multiparametric case of simultaneous misalignments and rotations of different kinds, has not been dealt with here. Nevertheless, the extension of the proposed procedures to these general situations can be made in a straightforward way.

Finally, let us point out that ocular aberrations are dependent on the accommodation state of the eye,[18] position across the visual field,[10] and wavelength[19] so that any static compensation procedure will degrade its performance if changes in the parameters for which it was designed occur. The influence of these factors on the degree of compensation achievable with a static single optical element remains as a subject for future research.

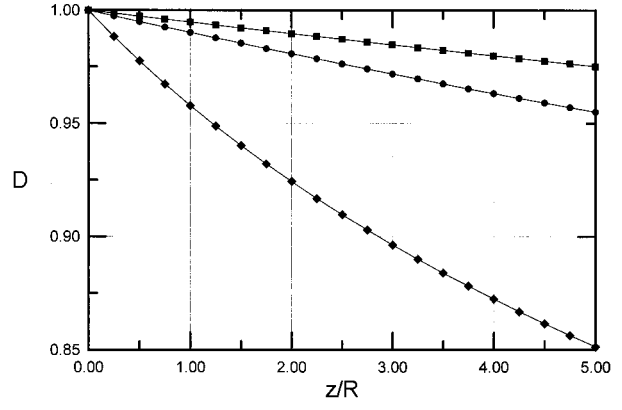

Fig. 6. Degree of compensation D versus normalized axial displacement z/R of the correcting plate for aberrations corresponding to subjects A (squares), B (circles), C (diamonds).

7. Conclusions

The compensation losses suffered when an otherwise perfect aberration-correcting plate is displaced either transversally or axially from its reference position or rotated in its own plane have been analyzed in this study. These losses are dependent on the kind and the amount of displacement and on the particular aberration pattern to be compensated for. The analytical and the numerical procedures presented here were applied to data of human eye aberrations including 35 Zernike terms up to the 7th radial and azimuthal degrees, measured with the laser ray-tracing method. For those cases, compensation efficiencies higher than 0.8 can be expected if the correcting plates are properly placed within 0.01 pu-

pil radius (laterally), ±7 deg (angularly), and several pupil radii (axially). These results suggest that lateral positioning, followed by angular positioning, are the key factors affecting compensation performance in practical setups, whereas axial positioning shows far less stringent requirements.

Aberration-correcting phase plates are manufactured at the Universidade de Santiago de Compostela. This study was supported by Spanish Comisión Interministerial de Ciencia y Tecnología grant (CICYT) TIC98-0925-C02-02.

References

1. N. López-Gil, H. C. Howland, B. Howland, N. Charman, and R. Applegate, "Generation of third-order spherical and coma aberrations by use of radially symmetrical fourth-order lenses," J. Opt. Soc. Am. A **15,** 2563–2571 (1998).
2. N. Chateau, A. Blanchard, and D. Baude, "Influence of myopia and aging on the optimal spherical aberration of soft contact lenses," J. Opt. Soc. Am. A **15,** 2589–2596 (1998).
3. J. Liang, D. R. Williams, and D. T. Miller, "Supernormal vision and high-resolution retinal imaging through adaptive optics," J. Opt. Soc. Am. A **14,** 2884–2892 (1997).
4. L. Zhu, P.-C. Sun, D.-U. Bartsch, W. R. Freeman, and Y. Fainmann, "Adaptive control of a membrane deformable mirror for aberration compensation," Appl. Opt. **38,** 168–176 (1999).
5. G. D. Love, "Wave-front correction and production of Zernike modes with a liquid-crystal spatial light modulator," Appl. Opt. **36,** 1517–1524 (1997).
6. F. Vargas-Martin, P. M. Prieto, and P. Artal, "Correction of the aberrations in the human eye with a liquid-crystal spatial light modulator: limits to performance," J. Opt. Soc. Am. A **15,** 2552–2562 (1998).
7. R. Navarro, E. Moreno-Barriuso, S. Bará, and T. Mancebo, "Phase plates for wave aberration compensation in the human eye," Opt. Lett. **25,** 236–238 (2000).
8. T. Mancebo, S. Bará, E. Moreno, and R. Navarro, "Single-mask photosculpted phase plates for the compensation of optical aberrations," in *Proceedings of Seventh International Microoptics Conference* (*MOC'99*) (Japan Society of Applied Physics, Tokyo, Japan, 1999), pp. 224–227.
9. R. Navarro and M. A. Losada, "Aberrations and relative efficiency of light pencils in the living human eye," Optom. Vis. Sci. **74,** 540–547 (1997).
10. R. Navarro, E. Moreno, and C. Dorronsoro, "Monochromatic aberrations and point-spread functions of the human eye across the visual field," J. Opt. Soc. Am. A **15,** 2522–2529 (1998).
11. D. Malacara and S. L. DeVore, "Interferogram evaluation and wavefront fitting," in *Optical Shop Testing*, D. Malacara, ed. (Wiley, New York, 1992), Chap. 13, pp. 455–499.
12. R. J. Noll, "Zernike polynomials and atmospheric turbulence," J. Opt. Soc. Am. **66,** 207–211 (1976).
13. M. Born and E. Wolf, *Principles of Optics* (Pergamon, Oxford, UK, 1980), Chap. 9, pp. 464–466.
14. M. Born and E. Wolf, *Principles of Optics* (Pergamon, Oxford, UK, 1980), Chap. 8, pp. 382–383.
15. J. J. Stamnes, *Waves in Focal Regions* (Hilger, Bristol, 1986), pp. 136–140.
16. J. Y. Wang and D. E. Silva, "Wave-front interpretation with Zernike polynomials," Appl. Opt. **19,** 1510–1518 (1980).
17. P. B. Liebelt, *An Introduction to Optimal Estimation* (Addison-Wesley, Reading, Mass., 1967), Chap. 5, pp. 135–159.
18. J. C. He, S. A. Burns, and S. Marcos, "Monochromatic aberrations in the accommodated human eye," Vision Res. **40,** 41–48 (2000).
19. S. Marcos, S. A. Burns, E. Moreno-Barriuso, and R. Navarro, "A new approach to the study of ocular chromatic aberrations," Vision Res. **39,** 4309–4323 (1999).